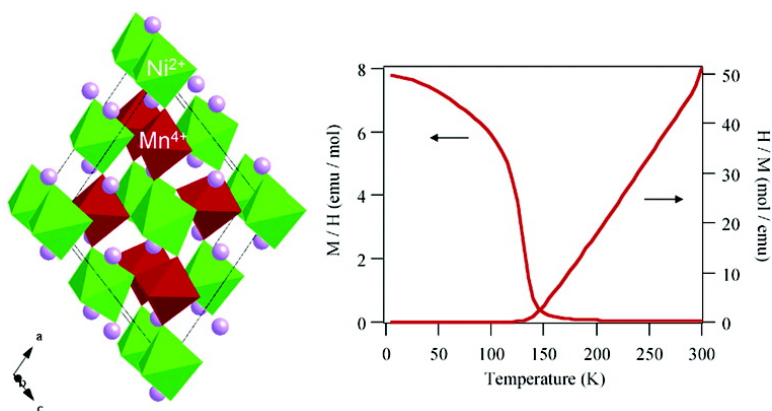


Designed Ferromagnetic, Ferroelectric BiNiMnO

Masaki Azuma, Kazuhide Takata, Takashi Saito, Shintaro Ishiwata, Yuichi Shimakawa, and Mikio Takano

J. Am. Chem. Soc., **2005**, 127 (24), 8889-8892 • DOI: 10.1021/ja0512576 • Publication Date (Web): 14 May 2005

Downloaded from <http://pubs.acs.org> on March 25, 2009



More About This Article

Additional resources and features associated with this article are available within the HTML version:

- Supporting Information
- Links to the 31 articles that cite this article, as of the time of this article download
- Access to high resolution figures
- Links to articles and content related to this article
- Copyright permission to reproduce figures and/or text from this article

[View the Full Text HTML](#)

Designed Ferromagnetic, Ferroelectric $\text{Bi}_2\text{NiMnO}_6$ Masaki Azuma,^{*,†,‡} Kazuhide Takata,[†] Takashi Saito,[†] Shintaro Ishiwata,^{†,§}
Yuichi Shimakawa,[†] and Mikio Takano[†]*Contribution from the Institute for Chemical Research, Kyoto University, Uji, Kyoto-fu 611-0011, Japan, and PRESTO, Japan Science and Technology Agency (JST), Kawaguchi, Saitama 332-0012, Japan*

Received February 28, 2005; E-mail: masaki@scl.kyoto-u.ac.jp

Abstract: A newly designed ferromagnetic, ferroelectric compound, $\text{Bi}_2\text{NiMnO}_6$, was prepared by high-pressure synthesis at 6 GPa. The crystal structure, as determined by synchrotron X-ray powder diffraction, is a heavily distorted double perovskite with Ni^{2+} and Mn^{4+} ions ordered in a rock-salt configuration. The presence of $6s^2$ lone pairs of Bi^{3+} ions and the covalent Bi–O bonds give ferroelectric properties with T_{CE} of 485 K, while $-\text{Ni}^{2+}-\text{O}-\text{Mn}^{4+}-\text{O}-\text{Ni}^{2+}-$ magnetic paths lead to a ferromagnetism with T_{CM} of 140 K. This simple material design to distribute two magnetic elements with and without e_g electrons on B sites of Bi- and Pb-based perovskites can be applied to other $\text{Bi}_2\text{M}^{2+}\text{M}^{4+}\text{O}_6$ and $\text{Pb}_2\text{M}^{3+}\text{M}^{5+}\text{O}_6$ systems to search for newer ferromagnetic ferroelectrics.

1. Introduction

A compound where magnetic and ferroelectric orders coexist is potentially of great use. If the coupling between magnetic and dielectric properties is strong enough to switch the direction of magnetization by application of an electric field, the thermal power of a magnetic memory will be drastically reduced. Discovery of anomalously large interplay between ferroelectricity and magnetism in TbMnO_3 ¹ and TbMn_2O_5 ² has accelerated such interest. Despite their usefulness, magnetic ferroelectrics are rare in nature and most of them are antiferromagnets with small responses to an external magnetic field. A classical way to obtain a magnetic ferroelectric is to locate Bi^{3+} or Pb^{2+} ions and a magnetic transition metal ion on A and B sites of a ABO_3 perovskite structure, respectively. The $6s^2$ lone pair of Bi (Pb) ions and the strong covalent character of Bi(Pb)–O bonds stabilize a noncentrosymmetric distorted structure.^{3,4} Indeed, BiFeO_3 is a well-known antiferromagnetic ($T_{\text{N}} = 643$ K) ferroelectric ($T_{\text{C}} = 1103$ K).⁵ Large spontaneous polarization and weak ferromagnetism due to a spin canting were recently reported in an epitaxial thin film of a tetragonal PbTiO_3 -type structure and stimulated many of the following works.⁶ BiMnO_3 ^{7–9} is the only ferromagnetic ($T_{\text{CM}} = 110$ K) ferroelec-

tric ($T_{\text{CE}} = 760$ K) among Bi,Pb-3d transition metal perovskites. High-pressure (HP) synthesis is a powerful tool to stabilize such distorted structures. HP syntheses of Bi,Pb-3d transition metal perovskites including BiMnO_3 were reported in the late 1960s.^{10–12} We have also investigated BiCrO_3 ,¹³ BiCoO_3 ,¹⁴ BiNiO_3 ,¹⁵ and PbVO_3 ,¹⁶ but these were all found to be antiferromagnets. The ferromagnetism of BiMnO_3 results from a particular orbital order. No other example of such an orbital order as the origin of the ferromagnetism is known. According to the Kanamori–Goodenough rules, a ferromagnetic insulator can also be obtained by distributing two kinds of transition metal ions with and without e_g electrons in a rock-salt configuration. Since no antiferromagnetic superexchange interaction mediated by oxygen ions works between the adjacent magnetic ions, ferromagnetic Hund's coupling is dominant. Such configuration is realized in La_2MMnO_6 with $\text{M} = \text{Co}$,^{17–19} Ni ,^{17,18,20} and

[†] Kyoto University.[‡] Japan Science and Technology Agency.[§] Present Address: Department of Chemistry, Princeton University, Princeton, NJ 08544.

- (1) Kimura, T.; Goto, T.; Shintani, H.; Ishizaka, K.; Arima, T.; Tokura, Y. *Nature* **2003**, *426*, 55–58.
- (2) Hur, N.; Park, S.; Sharma, P. A.; Ahn, J. S.; Guha, S.; Cheong, S.-W. *Nature* **2004**, *429*, 392–395.
- (3) Seshadri, R.; Hill, N. A. *Chem. Mater.* **2001**, *13*, 2892–2899.
- (4) Kuroiwa, Y.; Aoyagi, S.; Sawada, A.; Harada, J.; Nishibori, E.; Takata, M.; Sakata, M. *Phys. Rev. Lett.* **2001**, *87*, 217601–1–4.
- (5) Smolenskii, G. A.; Chupis, I. E. *Sov. Phys. Usp.* **1982**, *25*, 475–493.
- (6) Wang, J.; Neaton, J. B.; Zheng, H.; Nagarajan, V.; Ogale, S. B.; Liu, B.; Viehland, D.; Vaithyanathan, V.; Schlom, D. G.; Waghmare, U. V.; Spaldin, N. A.; Rabe, K. M.; Wuttig, M.; Ramesh, R. *Science* **2003**, *299*, 1719–1722.

- (7) Atou, T.; Chiba, H.; Ohoyama, K.; Yamaguchi, Y.; Syono, Y. *J. Solid State Chem.* **1999**, *145*, 639–642.
- (8) Moreira dos Santos, A.; Cheetham, A. K.; Atou, A.; Syono, Y.; Yamaguchi, Y.; Ohoyama, K.; Chiba, H.; Rao, C. N. R. *Phys. Rev. B* **2002**, *66*, 064425–1–4.
- (9) Kimura, T.; Kawamoto, S.; Yamada, I.; Azuma, M.; Takano, M.; Tokura, Y. *Phys. Rev. B* **2003**, *67*, 180401(R)–1–4.
- (10) Sugawara, F.; Iiida, S.; Syono, Y.; Akimoto, S. *J. Phys. Soc. Jpn.* **1968**, *25*, 1553–1558.
- (11) Tomashpol'skii, Yu. Ya.; Zubova, E. V.; Burdina, K. P.; Venevtey, Yu. N. *Sov. Phys. Crystallogr.* **1969**, *13*, 859–861.
- (12) Roth, W. L.; DeVries, R. C. *J. Appl. Phys.* **1967**, *38*, 951–952.
- (13) Niitaka, S.; Azuma, M.; Takano, M.; Nishibori, E.; Takata, M.; Sakata, M. *Solid State Ionics* **2004**, *172*, 557–559.
- (14) Niitaka, S.; Azuma, M.; Takano, M.; Nishibori, E.; Takata, M.; Sakata, M. *Meeting Abstracts of the Physical Society of Japan, 59th Annual Meeting, Kyushu University, March 27–30, 2004*, **2004**, *59*, Issue 1, Part 3 (ISSN 1342–8349), p 511.
- (15) Ishiwata, S.; Azuma, M.; Takano, M.; Nishibori, E.; Takata, M.; Sakata, M.; Kato, K. *J. Mater. Chem.* **2002**, *12*, 3733–3737.
- (16) Belik, A. A.; Azuma, M.; Saito, T.; Shimakawa, Y.; Takano, M. *Chem. Mater.* **2005**, *17*, 269–273.
- (17) Blasse, G. *J. Phys. Chem. Solids* **1965**, *26*, 1969–1971.
- (18) Bull, C. L.; Gleeson, D.; Knight, K. S. *J. Phys.: Condens. Matter* **2003**, *15*, 4927–4936.
- (19) Dass, R. I.; Goodenough, J. B. *Phys. Rev. B*, **2003**, *67*, 014401–1–9.

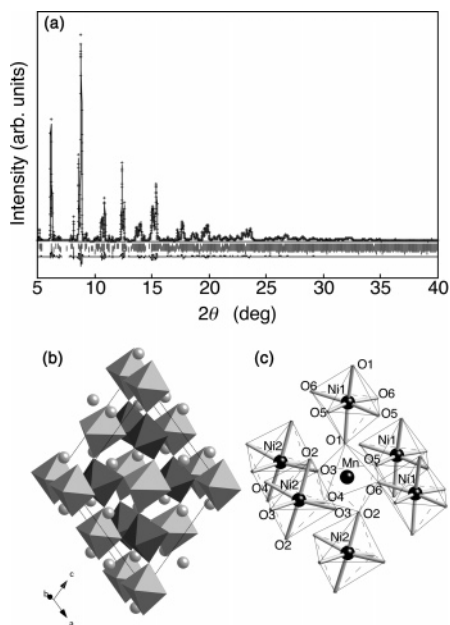


Figure 1. (a) Synchrotron X-ray powder diffraction pattern for $\text{Bi}_2\text{NiMnO}_6$. (b) Crystal structure of $\text{Bi}_2\text{NiMnO}_6$. Bright and dark octahedra correspond to NiO_6 and MnO_6 , respectively. (c) Linkage of NiO_6 and MnO_6 octahedra. The solid lines correspond to the occupied e_g orbitals.

Cu ,^{17,21} and these are indeed ferromagnets. $\text{Bi}_2\text{NiMnO}_6$ is thus expected to be a ferromagnetic ferroelectric, but no compound with this composition forms under ambient conditions.

We have succeeded in stabilizing this compound by means of HP synthesis. The crystal structure, as determined by synchrotron X-ray powder diffraction, is a heavily distorted double perovskite with Ni^{2+} and Mn^{4+} ions ordered in a rock-salt configuration, as intended. The presence of $6s^2$ lone pairs of Bi^{3+} ions and the covalent Bi–O bonds give ferroelectric properties with T_{CE} of 485 K, while $-\text{Ni}^{2+}-\text{O}-\text{Mn}^{4+}-\text{O}-\text{Ni}^{2+}$ –magnetic paths lead to a ferromagnetism with T_{CM} of 140 K.

2. Experimental Section

Bulk sample of $\text{Bi}_2\text{NiMnO}_6$ was prepared from a stoichiometric mixture of Bi_2O_3 , NiO , and MnO_2 . The starting material was charged into a gold capsule, treated at 6 GPa and 800 °C for 30 min in a cubic-anvil-type high-pressure apparatus. Then it was slowly cooled to the room temperature for 4–50 h before releasing the pressure. Synchrotron X-ray powder diffraction patterns were taken with a large Debye–Scherrer camera²² installed at BL02B2 of SPring-8 with $\lambda = 0.42098$ Å. The dielectric constant was measured with a LCR meter (Agilent 4284A). The measurement was conducted on heating in an oxygen flow to preserve the low conductivity. Magnetic susceptibility was measured with a SQUID magnetometer (Quantum Design MPMS XL) in a magnetic field of 100 Oe on cooling.

3. Results and Discussion

Figure 1a shows the synchrotron X-ray powder diffraction pattern taken at room temperature. The diffraction peaks could be indexed with a monoclinic unit cell of $a = 9.4646(4)$ Å, b

Table 1. Refined Structural Parameters for $\text{Bi}_2\text{NiMnO}_6$ at 300 K^a

atom	site	<i>x</i>	<i>y</i>	<i>z</i>	<i>B</i> (Å ²)
Bi1	4c	0.133(1)	-0.023(12)	0.378(1)	0.672(5)
Bi2	4c	0.369(1)	0.035(12)	0.123(1)	0.672
Ni1	2a	0	0	0	0.40(7)
Ni2	2b	0.5	0.015(2)	0.5	0.40
Mn	4c	0.243(3)	0.013(13)	0.749(3)	0.40
O1	4c	0.111(5)	-0.061(15)	0.849(6)	0.8
O2	4c	0.420(4)	0.042(14)	0.680(5)	0.8
O3	4c	0.146(9)	0.276(18)	0.636(9)	0.8
O4	4c	0.333(4)	0.242(14)	0.413(5)	0.8
O5	4c	0.377(5)	0.204(12)	0.899(5)	0.8
O6	4c	0.162(8)	0.216(17)	0.126(9)	0.8

^a Space group $C2$, $a = 9.4646(4)$ Å, $b = 5.4230(2)$ Å, $c = 9.5431(4)$ Å, and $\beta = 107.823(2)^\circ$. $R_{\text{wp}} = 4.79\%$ and $R_1 = 0.64\%$. ^b The same *B* values were given for Bi1 and Bi2, Ni, and Mn, respectively. The *B* value of O was fixed during the refinement.

Table 2. Ni–O and Mn–O Bond Lengths (Å) for $\text{Bi}_2\text{NiMnO}_6$

Ni1–O1	2.06(7) × 2	Mn–O4	2.10(5)
Ni1–O5	2.04(6) × 2	Mn–O5	1.90(5)
Ni1–O6	2.01(8) × 2	Mn–O6	2.05(8)
Mn–O1	1.83(7)	Ni2–O2	2.08(5) × 2
Mn–O2	1.99(6)	Ni2–O3	2.05(9) × 2
Mn–O3	1.85(9)	Ni2–O4	1.97(6) × 2

$= 5.4230(2)$ Å, $c = 9.5431(4)$ Å, and $\beta = 107.823(2)^\circ$. Since the unit cell was close to that of BiMnO_3 , a Rietveld structure refinement with the program RIETAN-2000²³ was performed by assuming a BiMnO_3 -type structure as an initial model. There are three transition metal sites, M1, M2, and M3, with multiplicities of 2, 4, and 2 in this structure. At the initial stage of the refinement, Ni^{2+} and Mn^{4+} were randomly distributed over these three sites. It was found that the M–O bond lengths were considerably shorter for the M2 site than M1 and M3 sites, so the small Mn^{4+} ion was assigned to the M2 site, and large Ni^{2+} ions were assigned to M1 and M3 at the final stage. Bond valence sums²⁴ calculated from the refined structural parameters were 2.14, 2.17, and 3.62 for Ni1, Ni2, and Mn ions, confirming the validity of this model. The determined crystal structure is shown in Figure 1b. Large Ni^{2+} octahedra and small Mn^{4+} octahedra are ordered in a rock-salt configuration, as expected. The refined structural parameters are summarized in Table 1. Figure 1c shows the linkage of NiO_6 and MnO_6 octahedra. Ni–O and Mn–O bond lengths are listed in Table 2. The NiO_6 and MnO_6 octahedra of $\text{Bi}_2\text{NiMnO}_6$ are rather isotropic reflecting the absence of a Jahn–Teller (J–T) distortion. This is in contrast with BiMnO_3 , where the O1–Mn1–O1, O3–Mn2–O6, and O2–Mn3–O2 bonds are longer than other O–Mn–O bonds by more than 10%, reflecting the electronic configuration of Mn^{3+} ions, $t_{2g}^3e_g^1$ ($S = 2$), and the ordering of the occupied e_g orbitals.^{7,8} The absence of the J–T distortion in NiO_6 and MnO_6 octahedra also supports the Ni^{2+} ($t_{2g}^6e_g^2$) and Mn^{4+} (t_{2g}^3) oxidation states in $\text{Bi}_2\text{NiMnO}_6$.

The $C2$ symmetry of this compound allows a spontaneous polarization along the *b* axis, and a calculation assuming a point-charge model with the above structural parameters gave a polarization of 20 $\mu\text{C}/\text{cm}^2$. The ferroelectric transition was observed by a dielectric constant measurement and also by a structural study. Figure 2 shows the temperature dependence of the relative dielectric constant. A peak was found at 485 K,

(20) Dass, R. I.; Yan, J.-Q.; Goodenough, J. B. *Phys. Rev. B* **2003**, *68*, 064415–1–12.

(21) Anderson, M. T.; Greenwood, K. B.; Taylor, G. A.; Poeppelmeier, K. R. *Prog. Solid State Chem.* **1993**, *22*, 197–233.

(22) Nishibori, E.; Takata, M.; Kato, K.; Sakata, M.; Kubota, Y.; Aoyagi, S.; Kuroiwa, Y.; Yamakata, M.; Ikeda, N. *Nucl. Inst. Methods Phys. Res. A* **2001**, *467–568*, 1045–1048.

(23) Izumi, F.; Ikeda, T. *Mater. Sci. Forum* **2000**, *321–324*, 198–203.

(24) Brown, I. D.; Altermatt, D. *Acta Crystallogr. Sect. B* **1985**, *41*, 244–247.

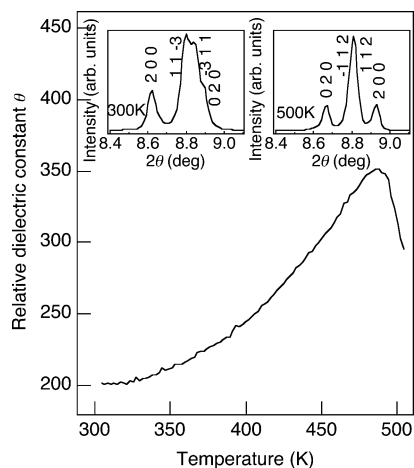


Figure 2. Temperature dependence of relative dielectric constant measured on heating at 10 kHz. The insets show portions of the powder XRD patterns taken at 300 and 500 K.

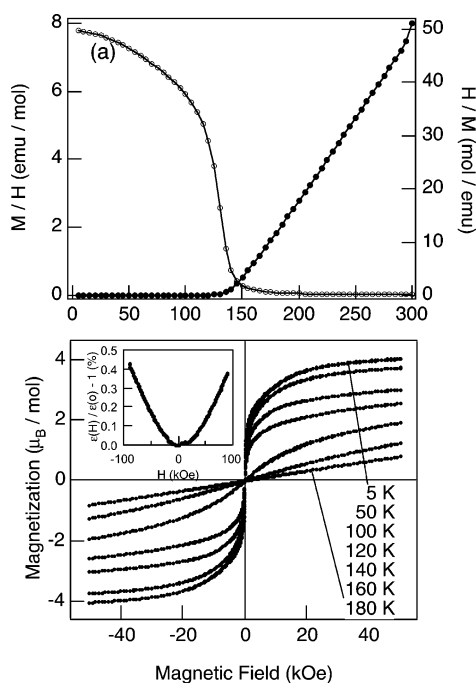


Figure 3. (a) Temperature dependences of magnetic susceptibility and inverse susceptibility of $\text{Bi}_2\text{NiMnO}_6$ measured in the external field of 100 Oe on cooling. (b) Magnetization of $\text{Bi}_2\text{NiMnO}_6$ measured at various temperatures. The inset shows the magnetic field dependence of the dielectric constant measured at 140 K and at 10 kHz.

suggesting the ferroelectric transition. Correspondingly, the crystal structure changed above T_{CE} . Insets of Figure 2 show portions of powder X-ray diffraction patterns. The pattern at 500 K was indexed with a monoclinic cell of $a = 5.4041(2)$ Å, $b = 5.5669(1)$ Å, $c = 7.7338(2)$ Å, and $\beta = 90.184(2)^\circ$. This $\sqrt{2}a \times \sqrt{2}a \times 2a$ monoclinic supercell of a cubic perovskite is the same as that of $\text{La}_2\text{NiMnO}_6$,¹⁸ where Ni^{2+} and Mn^{4+} are ordered in a rock-salt type configuration in a centrosymmetric (space group $P2_1/n$) structure. Rietveld refinement confirmed that the HT phase of $\text{Bi}_2\text{NiMnO}_6$ had the same centrosymmetric structure as $\text{La}_2\text{NiMnO}_6$. This phase transition from a centric GdFeO_3 type to acentric structure with $C2$ symmetry is the same as that of the well-known ferroelectric BiMnO_3 .⁹ Therefore, it is reasonable to regard $\text{Bi}_2\text{NiMnO}_6$ as a ferroelectric compound with $T_{\text{CE}} = 485$ K.

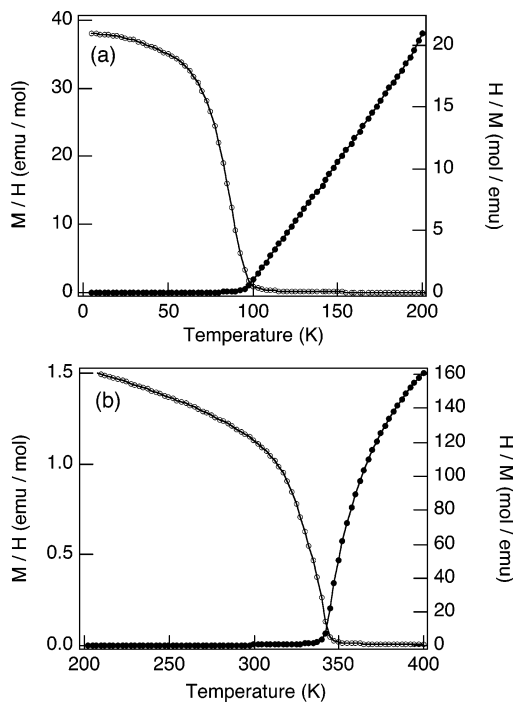


Figure 4. Temperature dependences of magnetic susceptibility and inverse susceptibility of $\text{Bi}_2\text{CoMnO}_6$ (a) and $\text{Bi}_2\text{CuMnO}_6$ (b) measured in an external field of 100 Oe on cooling.

As shown in Figure 1c, the MnO_6 octahedron is surrounded by 6 NiO_6 octahedra and vice versa, so the magnetic exchange path is $-\text{Ni}^{2+}-\text{O}-\text{Mn}^{4+}-\text{O}-\text{Ni}^{2+}$. Since a Ni^{2+} ion has the e_g^2 configuration while Mn^{4+} has no e_g electron, a ferromagnetic interaction is expected between the adjacent spins. Figure 3a shows the temperature dependence of the magnetic susceptibility measured on cooling in an external field of 100 Oe. The data exhibit a sharp increase at 140 K, indicating the ferromagnetic transition. As seen in the inverse $\chi-T$ plot in the same figure, the Weiss constant was 140 K, also confirming the ferromagnetic interactions between Ni and Mn spins. The magnetization measured at 5 K was $4.1 \mu_B$ at 5 T, as shown in Figure 3b. This value is close to $5 \mu_B$ expected from Ni^{2+} ($S = 1$) and Mn^{4+} ($S = 3/2$), but still smaller. This is probably due to a small antisite disorder of Ni^{2+} and Mn^{4+} ions. The resulting $\text{Ni}-\text{O}-\text{Ni}$ and $\text{Mn}-\text{O}-\text{Mn}$ magnetic paths give antiferromagnetic interactions and thus reduce the saturated magnetization. It should be noted that quenching from 1073 K after the HP synthesis before releasing the pressure resulted in the random mixing of Mn and Ni, and a substantial decrease of the ordered magnetic moment was observed.

The ratio of $T_{\text{CM}}/T_{\text{CE}}$ is 0.29 for the present system. This value is about twice that of BiMnO_3 , where the capacitance changed by 0.7% in an external magnetic field of 9 T at 100 K,⁹ so a more remarkable magnetoelectric effect is expected. Contrary to our expectation, the magnetic field induced capacitance change at 9 T shown in the inset of Figure 3b was 0.4% at $T_{\text{CM}} = 140$ K, even smaller than that of BiMnO_3 . This small change might be attributed to the partial disorder of Ni^{2+} and Mn^{4+} , as suggested by the magnetization measurement. In the case of BiMnO_3 , substitution of Cr for Mn rapidly suppressed the magnetocapacitance effect.

It should be emphasized that our material design of Bi- or Pb-based perovskites can be applied to other combinations of

transition metal ions with and without e_g electrons. Indeed, we have succeeded in synthesizing $\text{Bi}_2\text{CoMnO}_6$ and $\text{Bi}_2\text{CuMnO}_6$. These were found to be ferromagnets with a T_{CM} 's of 95 and 340 K, respectively, as seen in Figure 4. The saturation moment for $\text{Bi}_2\text{CoMnO}_6$ at 5 K was $3.5 \mu_{\text{B}}/\text{Co} + \text{Mn}$, considerably smaller than $6 \mu_{\text{B}}$ expected for $\text{Co}^{2+} + \text{Mn}^{4+}$. This indicates that the degree of the ordering is lower than that of $\text{Bi}_2\text{NiMnO}_6$. The saturation moment for $\text{Bi}_2\text{CuMnO}_6$ was even smaller, less than $1 \mu_{\text{B}}$. This value is comparable to that reported for $\text{La}_2\text{-CuMnO}_6$.¹⁷ The small saturation moments can be attributed to the difficulty in ordering anisotropic (Jahn–Teller) CuO_6 octahedra and isotropic MnO_6 octahedra.

In conclusion, we designed a new ferromagnetic, ferroelectric material, $\text{Bi}_2\text{NiMnO}_6$, and succeeded in its preparation and characterization. This metastable phase with noncentrosymmet-

ric, heavily distorted perovskite structure was stabilized by HP synthesis. Ordering of Ni^{2+} and Mn^{4+} ions with and without e_g electrons in a rock-salt configuration leads to the ferromagnetic interactions between the adjacent spins. This simple material design can be applied for other $\text{Bi}_2\text{M}^{2+}\text{M}'^{4+}\text{O}_6$ and $\text{Pb}_2\text{M}^{3+}\text{M}'^{5+}\text{O}_6$ systems.

Acknowledgment. The synchrotron radiation experiments were performed at the SPring-8 with the approval of the Japan Synchrotron Radiation Research Institute. The authors express their thanks to the Ministry of Education, Culture, Sports, Science and Technology, Japan, for Grants-in-Aid No. 14204070, No. 12CE2005 for COE Research on Elements Science, and for 21COE on the Kyoto Alliance for Chemistry.

JA0512576